Surface Science 606 (2012) 886–891

Contents lists available at SciVerse ScienceDirect

Surface Science

journal homepage: www.elsevier.com/locate/susc

First-principles study of the water structure on flat and stepped gold surfaces

Xiaohang Lin, Axel Groß *

Institut für Theoretische Chemie, Universität Ulm, 89069 Ulm/Germany

ARTICLE INFO

Article history:
Received 15 November 2011
Accepted 20 December 2011
Available online 28 December 2011

Keywords:
Water
Gold surfaces
Density functional theory calculations
Vibrational spectrum
Work function
Stepped surfaces

ABSTRACT

The geometric structure and electronic properties of flat and stepped gold–water interfaces have been addressed by periodic density functional theory (DFT) calculations. This work was motivated by a recent electron energy loss spectroscopy study [H. Ibach, Surf. Sci. 604 (2010) 377] indicating that the structure of a water layer on stepped Au(511) differs significantly from the one on Au(100). Based on ab initio molecular dynamics simulations, the measured spectra have been reproduced and linked to the geometric arrangement of the water molecules. Furthermore, we find a strong polarization of the water layers which contributes to the water-induced work function change of the substrate.

1. Introduction

The atomic level understanding of metal–water interfaces is of strong current interest [1–9], not only from a fundamental but also from an applied point of view, in particular in the context of electrochemistry, corrosion, and atmospheric science [10]. Stepped surfaces are particularly interesting [11–13] as they are present in any realistic surface and often exhibit specific electronic [13], chemical [14] and/or catalytic [15–17] properties. To systematically study the effects of steps on the properties of metal–water interfaces, vicinal surfaces are well-suited since they have a well-defined step structure.

Although the structure of water layers, especially the stratification of liquid water near electrode surfaces, has been studied intensively, for example by experiments using grazing incidence X-ray and scanning tunneling microscopy (STM) [10,18–23], still the structure of water at metal surfaces, in particular at structured surfaces remains unclear. On hexagonal densely-packed (111) substrates, usually it has been assumed that water forms crystalline ice-like layers because of the matching hexagonal geometry [18,19,24–29], however, recent ab initio molecular dynamics studies [6,30] have indicated that at temperatures above 150 K the water layers become disordered. On more strongly interacting metal substrates such as Ru Rh and Ni, water tends to form half-dissociated water-layers [7,27,31], however, their formation might be kinetically hindered [21].

At non-hexagonal or stepped surfaces, the situation is even less clear since these substrates do not support a hexagonal arrangement of the water molecules. The resulting structure will be a consequence of the balance between water–water and water–metal interactions which are of comparable strength [26,32,33] so that it is not trivial to make any structural predictions.

Recently, vibrational spectra of water adsorbed on Au(100), Au(511) and Au (11 1 1) were measured at low temperatures (140 K) using electron energy loss spectrometry (EELS) by H. Ibach [5]. This work was motivated by the observed large reduction of the Helmholtz capacitance or inner-layer capacitance on stepped gold and silver surfaces [13].

In single adsorbed water layers, not all hydrogen atoms of the water molecules can be hydrogen-bonded to other water molecules. For example, in the ice-like hexagonal bilayers on (111) substrates every second water molecule has a hydrogen atom pointing either up (H-up) or down towards the surface (H-down). These water structures have comparable energies, their stability depends on the particular substrate [6,27]. In vibrational spectra of water layers, the presence of the hydrogen-bonded (HB) hydrogen is reflected by a mode at about 3400 cm^{-1}, whereas non hydrogen-bonded (NHB) hydrogen leads to a peak at 3700 cm^{-1} [5,34]. The EELS spectra of water adsorbed on Au(100) at 140 K display in the O–H-stretch regime only a peak at 3390 cm^{-1}. The absence of the NHB hydrogen peak was taken as an evidence for a H-down water layer on Au(100) [5]. On stepped Au surfaces, on the other hand, significantly different vibrational spectra were found. Most importantly, the spectra contain a peak close to 3700 cm^{-1} which has been attributed to the presence of NHB hydrogens. Based on these findings, Ibach proposed three different structural models for a water layer on Au(511) involving distorted hexagonal rings which were all assumed to be consistent with the observed vibrational spectra [5]. However, a final assessment of the true water structure solely based on the vibrational spectra could not be made.

In the present work, we have addressed structural and electronic properties of water layers on Au(100) and Au(511) by performing

* Corresponding author. Tel.: +49 731 50 22810; fax: +49 731 50 22819.
E-mail address: axel.gross@uni-ulm.de (A. Groß).

0039-6028/$ – see front matter © 2011 Elsevier B.V. All rights reserved.
doi:10.1016/j.susc.2011.12.015

periodic density functional theory (DFT) calculations. The stability of several water structures has been evaluated. In addition, ab initio molecular dynamics (AIMD) simulations have been performed at temperatures of 140 K and 300 K in order to assess the thermal stability of the water layers and to derive vibrational spectra. Furthermore, we have analyzed the electronic structure of the water–Au systems.

2. Theoretical methods

All DFT calculations were performed using the Vienna ab initio simulation package (VASP) [35,36] within the generalized gradient approximation (GGA) to describe the exchange-correlation effects, employing the Perdew, Burke and Ernzerhof (PBE) exchange–correlation functional [37]. It has already been shown that this functional gives a reasonable description of water systems [6,38,39]. The plane-wave cutoff energy was set to 400 eV. The Au(100) was modeled by a 5 layer slab, whereas 15 layers were used for Au(511) with a vacuum region of 20 Å. The geometry of the water–metal systems was optimized by relaxing all atoms of the water layers and the uppermost two layers for Au(100) and the uppermost five layers for Au(511). The Au lattice constant was taken from the theoretical lattice parameter calculated for bulk gold (4.168 Å).

The adsorption energy per water molecule was determined according to

$$E_{ads} = \left(E_{tot} - E_{surf} - E_{water}\right)/N, \quad (1)$$

where E_{tot}, E_{surf} and E_{water} are the energies of the total water–metal system, the bare surface and the isolated water molecule, respectively. N is the number of water molecules per unit cell. The water structures were relaxed until the residual forces were smaller than 0.01 eV/Å using a 2×2 supercell for Au(100) and 2×2 and 2×3 supercells for Au(511), depending on the considered water structure. A k-point sampling of $5\times5\times1$ k-points was used to perform the integration over the first Brillouin zone. The convergence of the results with respect to these parameters has been carefully checked [40]. The AIMD simulations were performed within the microcanonical ensemble using the Verlet algorithm with a time step of 1 fs within a 2×2 supercell for Au(100) and a 1×3 supercell for Au(511). Thermal runs were carried out at temperatures of both 140 K and 300 K starting with the optimized geometries and performing the statistical averages after thermalization of the water layer. The vibrational spectrum of the water layer was derived from the Fourier transform of the velocity-velocity autocorrelation function [41].

3. Results and discussion

3.1. Geometry

First we address the water structure on the flat (100) surface. Water structures on (100) surfaces are significantly less frequently studied than water structures on the hexagonal (111) surfaces [10,19].

Au(100) surfaces prepared in ultrahigh vacuum are always reconstructed with the uppermost layer forming an incommensurate, approximately hexagonal structure [5,42]. Because of the difficulties associated with describing incommensurate structures within a periodic supercell approach, we have not made any attempt to model the reconstructed Au(100) surface. Rather, the results of Ibach for the Au(100) surface might be compared to simulations for water layers on Au(111) [6]. In contrast, the Au(511) surface which consists of (100) terraces does not reconstruct [43]. In order to have a reference for water on the (100) terraces, we consider a water layer on unreconstructed Au(100).

According to a DFT study using an Au_{12} cluster to model the Au(100) surface [44], an isolated water molecule is most strongly bound to bridge and on-top positions. However, to the best of our knowledge, except for the recent study of Ibach [5] there are no studies addressing the microscopic structure of water *layers* on Au(100). Water on Pt(100), on the other hand, has been the subject of a few studies [34,45,46]. Typically it has been assumed that water forms a rectangular structure with every surface atom covered by a water molecule on Pt(100) [45,46]. For Au(100), we have adopted a similar structure as our starting point. The optimized structure obtained within a 2×2 geometry assuming an H-down configuration is illustrated in Fig. 1. There are two inequivalent water molecules per unit cell, one with a hydrogen atom pointing down, the other one bound with the oxygen atom to the underlying Au atom. Still, the water structure is rather flat with the distance between oxygen atoms of the water molecules and the underlying Au atom being about 3.6 Å. Every water molecule is bonded to two neighboring water molecules with a O–O distance of 2.8 Å which is quite typical for the H-bonded oxygen atoms. The O–O distance to the other two neighboring water molecules is 0.5 Å larger so that they can be regarded as not being bonded. This results in a water structure formed by an H-bonded zigzag chain.

The choice of the water structures on Au(511) considered as the initial configurations for the structure optimization was motivated by the suggestions proposed by Ibach [5]. In addition, we tried several other structures. However, all these structures relaxed basically towards the structures shown in Fig. 1. The structures depicted in Fig. 1b and c possess a 1×3 periodicity whereas the structure in Fig. 1d corresponds to a 1×2 periodicity. The water coverage is the same in all structures with six (Fig. 1b and c) and four (Fig. 1d) water molecules per unit cell. The adsorption energies per water molecule are listed in Table 1. The most stable structure corresponds to the one shown in Fig. 1b but the one depicted in Fig. 1c is within the accuracy of our calculations practically degenerate.

These two structures are rather similar, they only differ in the position of the H-up water molecules. In the following, we concentrate on the structure shown in Fig. 1b which is in fact rather close to the one proposed by Ibach (Fig. 8a in Ref. [5]). It is formed by a

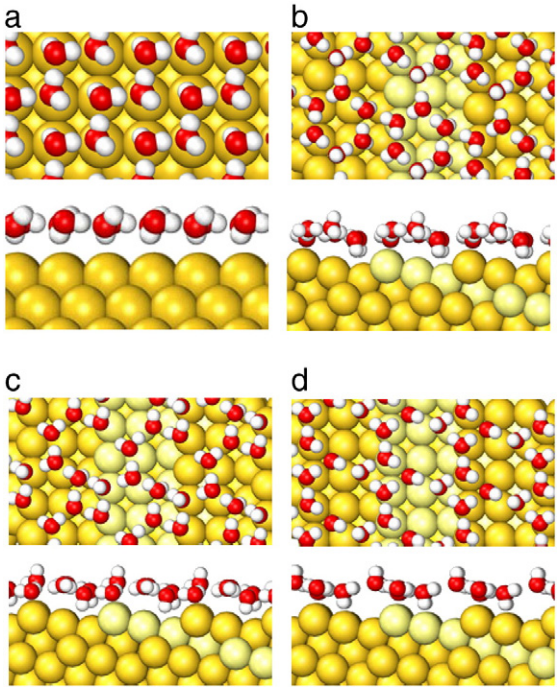

Fig. 1. Top and side view of the relaxed water structure on Au(100) (a) and Au(511) (b–d).

Table 1
Water adsorption energies in eV per H_2O molecule on Au(100) and on Au(511) for the structures illustrated in Fig. 1.

Structure	Au(100)	Au(511)b	Au(511)c	Au(511)d
E_{ads} (eV/H_2O mol.)	−0.391	−0.438	−0.431	−0.303

complete hexagon located on the (100)-like terraces. Hexagons of adjacent terraces are connected by distorted rectangles and octagons. Note that the water molecules at the lower step edge are in an H-down configuration. Thus the water layer can become rather smooth with all oxygen atoms located almost in one plane. The distances of the oxygen atoms to the underlying metal atoms are 3.30 Å, 4.17 Å and 3.84 Å, starting from the water adsorbed at the upper site of the step edge towards the one adsorbed at the lower site. The water molecules at the middle of the terrace are rather far away from the surface, even 0.33 Å further than those above the lower site of the step edge. Still, the height difference with respect to a (511) plane within the water layer of about about 0.3 Å is much smaller than the height difference between the uppermost substrate atoms (0.7 Å). Note that there is only one H-up and one H-down molecule per unit cell, the other water molecules are oriented more or less parallel to the surface. The average distance between the oxygen atoms of two neighboring water molecules on the same terrace is 2.78 Å, whereas it is enlarged to 3.13 Å across the step edge. Finally, the optimized water structure within the 1×2 geometry (Fig. 1d) is significantly less stable than the structures within the 1×3 geometry so that it is rather unlikely that it is realized.

3.2. Ab initio molecular dynamics simulations

Recently it has been shown that the observed work function change of metal surfaces upon the adsorption of a water layer can only be understood if a thermally induced random orientation of the water molecules is assumed [6]. In order to assess the stability of the water layers on Au(100) and Au(511) at finite temperatures and to derive the vibrational spectrum, AIMD simulations at 140 K and 300 K have been performed for a run time of 8 ps. Snapshots of the initial configuration and the final configuration at both temperatures are shown in Fig. 2.

On Au(100), the rectangular structure obviously dissolves at 140 K (see Fig. 2b). Instead, a more open hydrogen-bonded network of water molecules evolves with almost all water molecules oriented in a plane perpendicular to the (100) surface. At 300 K which is in fact above the desorption temperature of water monolayers from Au surfaces, the resulting structure becomes even more open, reflecting the fact that the adsorbed water layer is not thermodynamically stable at room temperature. The run time of the simulations has just not been long enough for the desorption to be completed.

The water structure on (100) surfaces certainly deserves further attention. However, here we rather focus on the water structure on stepped Au for which a proposal for a possible structure exists based on the limited width of the terraces. Interestingly enough, on Au(511) the water layer hardly changes its structure at 140 K, and even at room temperature, there is no indication of any structural rearrangement prior to desorption which sooner or later should occur at this temperature. In addition, there is no sizable reorientation of the water molecules which has been observed on (111) surfaces, also for more strongly interacting substrates such as Pt or Ru [6]. Single water molecules are only bound with an adsorption energy of −0.088 eV to the Au(100) surface which is even lower than the adsorption energy of −0.13 eV calculated for the water monomer bound to Au(111) [27]. At the lower step edge of the Au(511) surface, however, we find a much larger water monomer adsorption energy of −0.257 eV. Obviously, the water molecules strongly bound to the step edge atoms pin the water structure and lead to a high thermal stability of the water monolayer on Au(511).

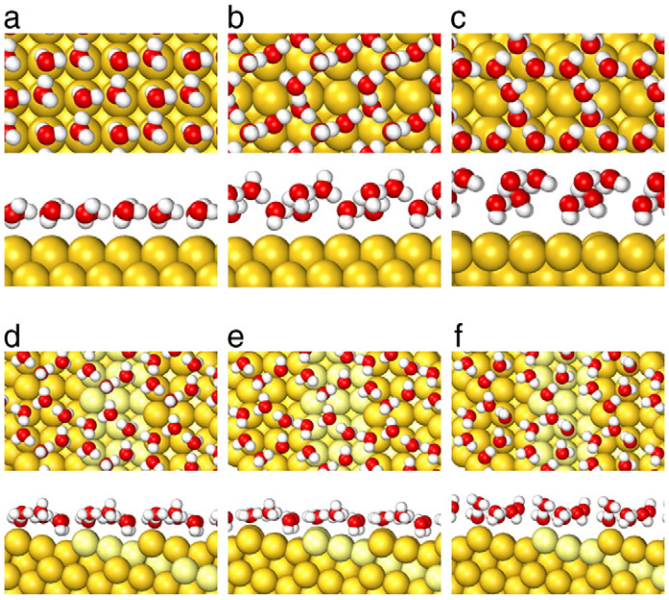

Fig. 2. Snapshots of the AIMD simulations on Au(100) (a,b,c) and Au(511) (d,e,f) in top and side view. Panels a and d: initial conditions; b and e: $t=8$ ps, $T=140$ K; c and f: $t=8$ ps, $T=300$ K.

As mentioned above, the oxygen atoms of the water molecules at the upper side of the steps are located much closer to the Au atoms than the oxygen atoms above the terrace sites. This means that the interaction of these water molecules at the terraces with the underlying Au atoms is much weaker. This much weaker binding might then conversely lead to a stronger water–water binding. Thus it is very likely that in total the thermal stability of the water layers at Au(511) is caused by the pinning of the water molecules at the steps together with the weaker metal–water and the stronger water–water interaction above the terraces.

Since snapshots can sometimes be deceiving, in Fig. 3 we have plotted the trajectories of the oxygen atoms of the water molecules along the AIMD runs at 140 K on Au(100) and Au(511). The trajectories confirm the picture already derived from Fig. 2: on Au(100), there is a substantial restructuring of the water layer whereas on Au(511) the water molecules are rather stationary, in particular those at the step edge.

Using the Fourier transform of the velocity auto-correlation function, we derived the vibrational spectrum of the water layers on Au(100) and Au(511) in order to allow for a direct comparison with the experiment [5]. In order to reduce the dependence of the calculated spectra from the initial conditions, the results shown in

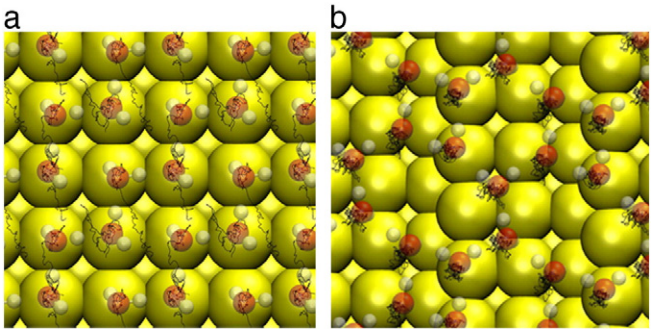

Fig. 3. Trajectories of the oxygen atoms of the water molecules indicated by the dark lines derived from the AIMD simulations at 140 K on Au(100) (a) and Au(511) (b).

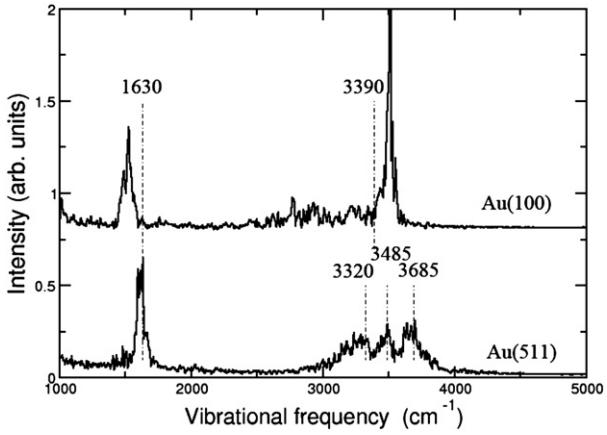

Fig. 4. Calculated vibrational spectra of the water layer on Au(100) and Au(511) derived from the Fourier transform of the velocity auto-correlation function. Experimentally observed modes [5] are indicated by dashed lines.

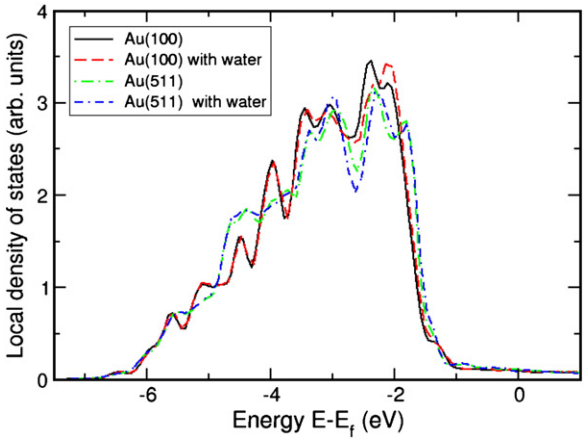

Fig. 5. Local density of states (LDOS) of the d-states of a Au atom in the uppermost layer of Au(100) and Au(511) in the absence and the presence of a water layer in the energy minimum structures.

Fig. 4 have been averaged over five different configurations after the thermalization of the water layer was completed.

One of the prominent features observed in the experiments is a hydrogen scissor mode at 1630 cm^{-1} on both Au(100) and Au(511). In the O–H stretch regime, on Au(100) there is a single mode at 3390 cm^{-1}, whereas three modes have been identified on Au(511), two stretching modes at 3320 cm^{-1} and 3485 cm^{-1} which have been attributed to H-bonded (HB) hydrogen, and a stretching mode at 3685 cm^{-1} associated with non-H-bonded (NHB) hydrogen [5]. These modes are indicated as dashed lines in Fig. 4.

On Au(100), we find two sharp features in the calculated vibrational spectrum at about 1600 cm^{-1} and 3500 cm^{-1} which are related to the hydrogen scissor mode and O–H stretching mode, respectively. Interestingly enough, in spite of the rather open structure of the water layer (see Fig. 2b) with hydrogen atoms being non-bonded and bonded both to Au and to oxygen atoms, there is only one distinct peak in the O–H stretch region. The frequencies of the non-H-bonded hydrogen atoms might be red-shifted, as already suggested to explain the experimental results with only one peak in the O–H stretching region [5]. Note that AIMD simulations of water on Au(111) performed at 300 K yield similar results as those obtained here for Au(100), namely one hydrogen scissor mode at about 1600 cm^{-1} and also only one broad peak centered around about 3500 cm^{-1} [6].

Although DFT-derived vibrational frequencies often exhibit discrepancies compared to the experiment [47], the fact that both a red-shift and a blue-shift are obtained indicates that water on Au(111) might be not an appropriate model to describe water on reconstructed Au(100).

For Au(511), on the other hand, there is a rather good agreement between measured and calculated water vibrational frequencies. This agreement might to a certain degree be fortuitous. Furthermore, it should be noted that the height of the peaks do not agree with the experiment which is not surprising considering the fact that we have not included the dipole selection rules in the simulation of the vibrational spectra. Still, the fact that the hydrogen scissor mode as well as the three-fold splitting of the O–H stretch mode is qualitatively and quantitatively reproduced indicates that the structural model for the water layer on Au(511) illustrated in Fig. 1b should be correct.

3.3. Electronic properties

In order to obtain a deeper understanding of the properties of water layers on Au(100) and Au(511) we have also analyzed their electronic structure. In Fig. 5, the d-band local density of states (LDOS) is plotted for a Au atom in the uppermost layer of Au(100) and Au(511) in the absence and the presence of a water layer where the energy minimum structures of water depicted in Figs. 2a and d have been used. Note that on clean Au(511) and in the presence of water there are inequivalent surface atoms. In order to keep Fig. 5 clearly laid out, we have selected one specific surface atom for both Au(100) and Au(511), namely one located below a hydrogen atom, however, the findings for the other surface atoms are rather similar. Fig. 5 in fact confirms what has already been found in the case of water layers on Pt(111) [6,28]. Because of the relatively weak interaction between water molecules and metal atoms, the LDOS of the metal surface is hardly influenced by the presence of water.

In spite of the small change in the LDOS of the metal substrate, there is still a significant polarization of the water molecules upon the adsorption of the water layer [6]. This is illustrated in Fig. 6 where isosurfaces of the charge density differences upon water adsorption on Au(100) and Au(511) are plotted. On Au(100), there is a particular strong charge accumulation of electron density below the water molecule being oriented parallel to the surface and bound via the oxygen atom to the Au atom whereas there is a considerable charge depletion below the H-down water molecule (Fig. 6c). On Au(511), the charge rearrangement is mainly localized at the step edge, however, qualitatively a similar pattern of charge depletion and accumulation as on Au(100) arises (Fig. 6d). This charge rearrangement also contributes to the water-induced work function change.

In Table 2, the work function of clean and water-covered Au(100) and Au(511) is listed together with the water-induced work function change $\Delta\Phi$ which corresponds to the difference of these two values. Experimentally, for Au(100) a work function of 5.22 ± 0.04 eV was measured [48]; our calculated value of 5.022 eV compares reasonably well with the experiment. However, the calculated water-induced work function changes of −0.093 eV and −0.057 eV for Au(100) and Au(511), respectively, seem at first sight to be surprisingly small considering the large polarization of the water layers just discussed. In order to understand this result one has to take into account that both water layers correspond to H-down layers, i.e. the water molecules not oriented parallel to the surface bind with their hydrogen atom to the surface. In the water layer on Au(511), there is also one H-up water molecule but two H-down water molecules per unit cell. H-down water layers have an intrinsic dipole moment that would increase the work function [6]. The fact that we find slight work function decreases upon the water adsorption indicates that the intrinsic water dipole moment is overcompensated by the strong polarization of the water layers illustrated in Fig. 6. Similar results have been found for water layers adsorbed on strongly interacting hexagonal substrates such as Ru(0001) [6].

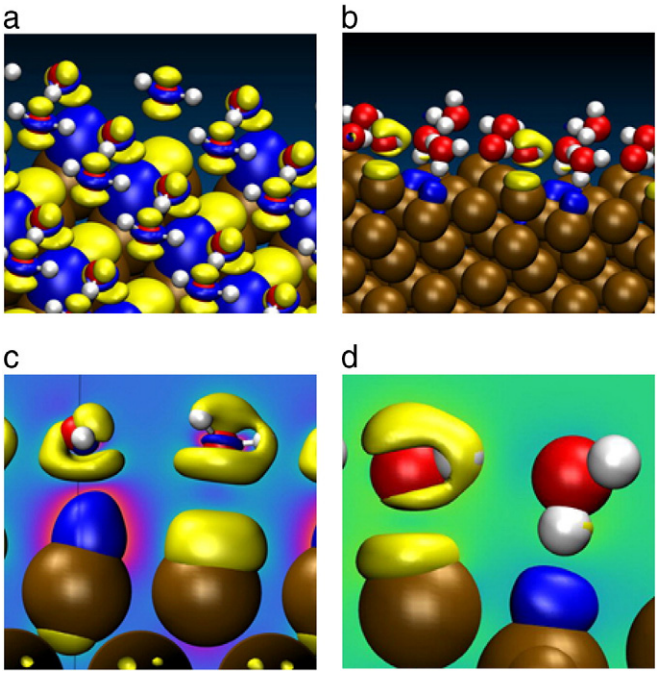

Fig. 6. Isosurface plots of charge density differences upon water adsorption on Au(100) (panels a and c, value 0.004 $e/Å^3$) and Au(511) (panels b and d, value 0.009 $e/Å^3$). Charge accumulation, i.e. accumulation of electron density, is plotted in yellow, charge depletion in blue. In contrast to the previous figures, the Au atoms are colored in brown. Panels c and d show a close-up of the regions with the largest charge rearrangement.

At stepped Au and Ag surfaces, a reduced Helmholtz capacitance has been found compared to the corresponding flat surfaces [13]. It has been speculated that this reduction is due to a lower polarizability of the water molecules at the steps [13]. Now we have not performed any calculations for varying external electric fields or electrode potentials which is beyond the scope of the present paper; hence we cannot directly derive any facts with respect to the polarizability of the water layers. Still it is interesting to note that according to Fig. 6b on Au(511) the water layers are only polarized close to the steps. The water molecules above the terraces hardly show any polarization which can be related to the fact that their position is further away from the metal atoms so that they are only weakly interacting with the substrate. On unreconstructed Au(100), on the other hand, all water molecules in the first water layer are strongly polarized (see Fig. 6a).

It is now tempting to assume that the polarizability of the water molecules is related to the strength of their interaction with the metal substrate. Hence it might well be that not the water molecules at the steps exhibit the smaller polarizability but rather the water molecules above the terraces which are located further away from the metal atoms. A definite statement, however, can only be made after the polarizability of the water molecules has been explicitly determined.

Table 2
Work function in eV of clean and water-covered Au(100) and Au(511) and water-induced work function change $\Delta\Phi$.

Surface	Φ(Au)	$\Phi(H_2O/Au)$	$\Delta\Phi$
Au(100)	5.022	4.929	−0.093
Au(511)	5.041	4.984	−0.057

4. Conclusions

The structural, electronic and vibrational properties of a water layer on Au(100) and Au(511) have been studied by first principles total-energy calculations and ab initio molecular dynamics simulations. On Au(100) a structural model based on a (2×2) surface unit cell seems to be not realistic.

We obtained the most stable structures on Au(100) and Au(511). From the calculated vibrational spectra, several fundamental aspects have been derived. On Au(100), an OH stretching mode can be found at 3500 cm^{-1} and no NHB hydrogen stretching mode was obtained which might be caused by the weak interaction between water layers and the Au(100) surface. On Au(511), three peaks can be found around 3500 cm^{-1} (3300 cm^{-1}, 3500 cm^{-1} and 3600 cm^{-1}), where the appearance of two HB hydrogen stretching modes might be caused by the influence of the step edge. The simulation results with respect to the positions of the peaks agree with the experimental data quite well.

AIMD simulations show that at 140 K on Au(100) the rectangular structure is thermodynamically not stable whereas on Au(511) the calculated structure is quite stable. The charge density difference shows a rather localized and strong polarization of water at the step edge on Au(511). All of the phenomena indicate a strong interaction between step edge and water layer, and rather different electronic properties compared with the flat gold surface.

Acknowledgments

Financial support by the Baden-Württemberg-Stiftung tugh the network “Functional Nanostructures” is gratefully acknowledged. Computer time has been provided by the BW-Grid of the federal state of Baden-Württemberg and by a computer cluster financed through the stimulus programme “Electrochemistry for Electromobility” of the German Ministry of Education and Science (BMBF).

References

[1] R. Guidelli, W. Schmickler, Electrochim. Acta 45 (2000) 2317.
[2] K. Andersson, A. Nikitin, L.G.M. Pettersson, A. Nilsson, H. Ogasawara, Phys. Rev. Lett. 93 (2004) 196101.
[3] C. Clay, S. Haq, A. Hodgson, Chem. Phys. Lett. 388 (2004) 89.
[4] D.N. Denzler, C. Hess, R. Dudek, S. Wagner, C. Frischkorn, M. Wolf, G. Ertl, Chem. Phys. Lett. 376 (2003) 618.
[5] H. Ibach, Surf. Sci. 604 (2010) 377.
[6] S. Schnur, A. Groß, New J. Phys. 11 (2009) 125003.
[7] P.J. Feibelman, Science 295 (2002) 99.
[8] X. Wu, A.K. Ray, Phys. Rev. B: Condens. Matter 65 (2002) 085403.
[9] A. Michaelides, K. Morgenstern, Nat. Mater. 6 (2007) 597.
[10] A. Hodgson, S. Haq, Surf. Sci. Rep. 64 (2009) 381.
[11] Y. Tiwary, K.A. Fichthorn, Phys. Rev. B: Condens. Matter 81 (2010) 195421.
[12] J.E. Goose, E.L. First, P. Clancy, Phys. Rev. B: Condens. Matter 81 (2010) 205310.
[13] G. Beltramo, M. Giesen, H. Ibach, Electrochim. Acta 54 (2009) 4305.
[14] M. Lischka, A. Groß, Phys. Rev. B: Condens. Matter 65 (2002) 075420.
[15] S. Dahl, A. Logadottir, R.C. Egeberg, J.H. Larsen, I. Chorkendorff, E. Törnqvist, J.K. Nørskov, Phys. Rev. Lett. 83 (1999) 1814.
[16] A. Groß, J. Comput. Theor. Nanosci. 5 (2008) 894.
[17] H. Baltruschat, S. Ernst, ChemPhysChem 12 (2011) 56.
[18] P.A. Thiel, T.E. Madey, Surf. Sci. Rep. 7 (1987) 211.
[19] M.A. Henderson, Surf. Sci. Rep. 46 (2002) 1.
[20] M. Ito, M. Yamazaki, Phys. Chem. Chem. Phys. 8 (2006) 3623.
[21] S. Haq, C. Clay, G.R. Darling, G. Zimbitas, A. Hodgson, Phys. Rev. B: Condens. Matter 73 (2006) 115414.
[22] X. Wei, B. Miranda, Y.R. Shen, Phys. Rev. Lett. 86 (2001) 8.
[23] K. Andresson, A. Gomez, C. Glover, D. Nordlund, H. Oestroem, T. Schiros, O. Takahashi, H. Ogasawara, L.G.M. Pettersson, A. Nilsson, Surf. Sci. 585 (2005) 183.
[24] S. Meng, L.F. Xu, E.G. Wang, S. Gao, Phys. Rev. Lett. 89 (2002) 176104.
[25] S. Meng, E.G. Wang, S. Gao, Phys. Rev. B: Condens. Matter 69 (2004) 195404.
[26] A. Roudgar, A. Groß, Chem. Phys. Lett. 409 (2005) 157.
[27] A. Michaelides, Appl. Phys. A 85 (2006) 415.
[28] Y. Gohda, S. Schnur, A. Groß, Faraday Discuss. 140 (2008) 233.
[29] J. Kucera, A. Groß, Beilstein J., Nanotechnology 2 (2011) 384.
[30] S. Schnur, A. Groß, Catal. Today 165 (2011) 129.
[31] G. Materzanini, G.F. Tantardini, P.J.D. Lindan, P. Saalfrank, Phys. Rev. B: Condens. Matter 71 (2005) 155414.

[32] A. Michaelides, A. Alavi, D.A. King, J. Am. Chem. Soc. 125 (2003) 2746.
[33] A. Roudgar, A. Groß, Surf. Sci. 597 (2005) 42.
[34] H. Ibach, S. Lehwald, Surf. Sci. 91 (1980) 187.
[35] G. Kresse, J. Furthmüller, Phys. Rev. B: Condens. Matter 54 (1996) 11169.
[36] G. Kresse, J. Furthmüller, Comput. Mater. Sci. 6 (1996) 15.
[37] J.P. Perdew, K. Burke, M. Ernzerhof, Phys. Rev. Lett. 77 (1996) 3865.
[38] P. Vassilev, C. Hartnig, M.T.M. Koper, F. Frechard, R.A. van Santen, J. Chem. Phys. 115 (2001) 9815.
[39] J. VandeVondele, F. Mohamed, M. Krack, J. Hutter, M. Sprik, M. Parrinello, J. Chem. Phys. 122 (2005) 014515.
[40] P. Cabrera-Sanfelix, D. Sanchez-Portal, A. Mugarza, T.K. Shimizu, M. Salmeron, A. Arnau, Phys. Rev. B: Condens. Matter 76 (2007) 205438.
[41] M. Schmitz, P. Tavan, J. Chem. Phys. 121 (2004) 12247.
[42] B.M. Ocko, D. Gibbs, K.G. Huang, D.M. Zehner, S.G.J. Mochrie, Phys. Rev. B: Condens. Matter 44 (1991) 6429.
[43] M. Sotto, J. Boulliard, Surf. Sci. 214 (1989) 97.
[44] A. Ignaczak, J. Gomes, J. Electroanal. Chem. 420 (1997) 209.
[45] X. Xia, M.L. Berkowitz, Phys. Rev. Lett. 74 (1995) 3193.
[46] I.-C. Yeh, M. Berkowitz, J. Electroanal. Chem. 450 (1998) 313.
[47] I.S. Ulusoy, Y. Scribano, D.M. Benoit, A. Tschetschetkin, N. Maurer, B. Koslowski, P. Ziemann, Phys. Chem. Chem. Phys. 13 (2011) 612.
[48] G.V. Hansson, S.A. Flodström, Phys. Rev. B: Condens. Matter 18 (1978) 1572.